PROCEEDINGS, Thirty-Fifth Workshop on Geothermal Reservoir Engineering
Stanford University, Stanford, California, February 1-3, 2010
SGP-TR-188

THERMAL SINGLE-WELL INJECTION-WITHDRAWAL TRACER TESTS FOR DETERMINING FRACTURE-MATRIX HEAT TRANSFER AREA

Karsten Pruess and Christine Doughty

Earth Sciences Division, Lawrence Berkeley National Laboratory, Berkeley, CA 94720, USA
K_Pruess@lbl.gov

ABSTRACT

Single-well injection-withdrawal (SWIW) tracer tests involve injection of traced fluid and subsequent tracer recovery from the same well, usually with some quiescent time between the injection and withdrawal periods. SWIW are insensitive to variations in advective processes that arise from formation heterogeneities, because upon withdrawal, fluid parcels tend to retrace the paths taken during injection. However, SWIW are sensitive to diffusive processes, such as diffusive exchange of conservative or reactive solutes between fractures and rock matrix. This paper focuses on SWIW tests in which temperature itself is used as a tracer. Numerical simulations demonstrate the sensitivity of temperature returns to fracture-matrix interaction. We consider thermal SWIW response to the two primary reservoir improvements targeted with stimulation, (1) making additional fractures accessible to injected fluids, and (2) increasing the aperture and permeability of pre-existing fractures. It is found that temperature returns in SWIW tests are insensitive to (2), while providing a strong signal of more rapid temperature recovery during the withdrawal phase for (1).

INTRODUCTION

Development of enhanced geothermal systems (EGS) in rocks with insufficient natural permeability and fluid content requires stimulation, a treatment that involves injection of aqueous fluids at near-ambient temperatures and high pressures to enhance permeability and improve the flow and heat transfer characteristics of the reservoir. Such improvements arise from a combination of hydraulic effects (pressurization), mechanical changes (shear movement along pre-existing fracture planes that increases fracture permeability and porosity), chemical interactions between rocks and fluids that can dissolve and precipitate rock minerals, and thermal effects, including thermal contraction and thermal stress cracking (Kohl et al., 1995; Kohl and Mégel, 2007; Xu et al., 2009). In Iceland it is common practice to "finish off" drilling of a geothermal well with a stimulation treatment that involves cold water injection over time periods from days to a couple of weeks (Tulinius et al., 1996; Bjornsson, 2004). In order to design and optimize stimulation treatments, methods are needed for characterizing and quantifying the results of stimulation treatments in terms of enhanced permeability of the fracture network, and exposure of additional rock surface for heat transfer to injected fluids circulating in the fractures (Nalla and Shook, 2005). Permeability changes may be evaluated by means of flow tests and repeat pressure transient tests, in which the time dependence of injection pressures in response to applied injection rates is monitored. Enhancements in fracture-matrix heat transfer areas from stimulation treatments cannot be assessed by such flow tests. Additional characterization of reservoir properties, and assessment of the success of stimulation treatments, may be achieved through testing with conservative or reactive tracers. The most common tracer test involves injection of aqueous solutes into one or more injection wells, and monitoring of tracer returns in fluids produced from offset production wells (Shook, 2001; Sanjuan et al., 2006). Interdiffusion of solute tracers between fractures and rock matrix produces characteristic tails in tracer breakthrough curves (BTC), that may permit determination of fracture-matrix interface areas (Pruess, 2002; Pruess et al., 2005; Shan and Pruess, 2005).

One disadvantage of interwell tracer tests is that tracer breakthrough at offset observation wells may be weak and slow, requiring fluid sampling over extended time periods of weeks or even months. Also, suitable observation wells may not always be available. A possible alternative involves single-well injection-withdrawal (SWIW) tests, variously referred to as "huff and puff," "push-pull" or "injection-backflow" tests, in which fluid with tracer is injected into a well and, after some quiescent or rest period, is produced out of the same well (Kocabas and Horne, 1987; Haggerty et al., 2001; Nalla and Shook, 2005; Ghergut et al., 2006, 2009; Neretnieks, 2007). One potentially attractive feature of SWIW tests as compared to interwell tracer tests

(ITT) is the typically much shorter test duration, hours to a few days for SWIW as compared to weeks or months for ITT. This holds out the promise of obtaining test results much more quickly, providing significant economic benefits. Another potential advantage is that SWIW are much less affected than ITT by heterogeneities of flow in the fracture network, potentially providing a clearer signal of fracture-matrix interaction parameters such as "flow wetted surface area" (FWS), the all-important interface area between flowing fractures and wall rocks of low permeability (Neretnieks and Moreno, 2003; Doughty and Tsang, 2009). FWS is the critical parameter that determines achievable rates of rocks-to-fluid heat transfer, and thereby the productive capacity of the EGS reservoir. The region investigated by SWIW tests may be on the order of 5–50 m for test durations from hours to a few days.

This paper explores possibilities for characterizing properties of fractured reservoirs by means of "thermal" SWIW tests, in which temperature changes rather than solute concentrations are used as tracer. This would involve injecting cold water into a hot fracture, followed by a quiescent period during which this water would be heated by conduction from the wall rocks, and followed by backflow with temperature monitoring. The observed temperature rise during backflow will depend on the heat transfer area per unit injected volume of cold water, and may allow an estimation of heat transfer area. Using temperature as a tracer may have advantages over reactive or non-reactive solute tracers, including (1) temperature effects depend directly on heat exchange between fractures and matrix, the essential process of heat mining that we aim to characterize; (2) heat conduction is a diffusive process that is very "robust," depending as it does only on thermal parameters of rocks and fluids, whereas solute diffusion is sensitive to tortuosity effects that may be difficult to characterize and add uncertainty to interpretation; (3) thermal diffusivities of rocks are of order 10^{-6} m^2/s, three orders of magnitude larger than typical solute diffusivities (four to five orders larger when considering tortuosity effects in rocks of low permeability), suggesting that effects of fracture-matrix exchange may be much stronger than for solute tracers; (4) local heat exchange between fluids and rocks is analogous to reversible linear sorption of solute tracer, but the process depends only on robust thermal parameters, not on highly heterogeneous and difficult-to-characterize mineral abundances and surfaces as for sorbing solutes.

NUMERICAL SIMULATIONS

The purpose of this initial set of simulation runs is to demonstrate the sensitivity of temperature during backflow to the available fracture-matrix interface area. For simplicity we consider a vertically oriented homogeneous fracture with 1-D linear flow geometry. The basic geometric arrangement is shown in Fig. 1.

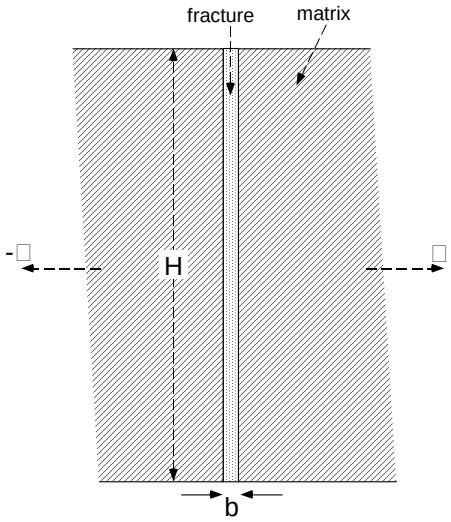

Figure 1: Schematic of a fracture with width b and height H and attached semi-infinite wall rocks.

The fracture is modeled as a porous domain with large permeability ($5x10^{-12}$ m^2) and porosity (50 %). We do not invoke a parallel-plate model for the fracture (Witherspoon et al., 1980); instead, we consider fracture walls to be rough, we allow for the presence of minerals in the fracture itself, and we include some wall rock into the fracture domain. Thermal equilibration within a fracture domain of a few centimeters width is rapid on the time scale of a typical SWIW test (hours to days), typically requiring only a few minutes (see Fig. 2). The value used for

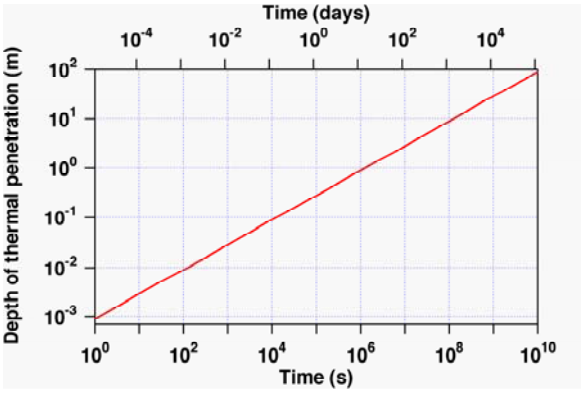

Figure 2: Depth of thermal penetration as function of time, for a typical rock thermal diffusivity of $0.8x10^{-6}$ m^2/s.

permeability is somewhat arbitrary. Permeability was chosen sufficiently large to limit the pressurization arising from fluid injection, and for the simulations

presented below, pressure increase at the injection point was less than 2 bar.

Thermal parameters are a formation conductivity of K = 2.1 W/m/°C, rock specific heat of c_R = 1000 J/kg/°C, and a rock grain density ρ_R = 2650 kg/m^3, corresponding to a thermal diffusivity of $D_{th} = K/\rho_R c_R = 0.793 \times 10^{-6}$ m^2/s. Bodvarsson (1972) showed that, for non-isothermal flow subject to instantaneous thermal equilibration between fluids and rock grains, the advancement of the thermal front is retarded relative to the hydrodynamic front by a thermal retardation factor R_{th}, which may be written as

$$R_{th} = \frac{\phi\rho_w c_w + (1-\phi)\rho_R c_R}{\phi\rho_w c_w} \qquad (1)$$

where ϕ is porosity, ρ is density, c is specific heat, and the subscripts w and R denote water and rock, respectively. From the parameters given above and using $\rho_w \approx 1000$ kg/m^3, $c_w \approx 4000$ J/kg/°C, the thermal retardation factor for a porosity ϕ = 50 % can be estimated from Eq. (1) as R_{th} = 1.66. Initial conditions are a temperature of 200 °C and a pressure of 200 bar.

A 1-D computational grid was used that is oriented perpendicular to the "elevation view" shown in Fig. 1. The grid consists of 1,000 blocks of 1 cm thickness each, for a total length of 10 m. We consider fractures of different height H and width b, but maintain the cross-sectional area in the direction perpendicular to flow constant at bH = 1 m^2. Water in the amount of 3,600 kg is injected at a temperature of 20 °C at a constant rate of 0.2 kg/s for a period of 5 hours. Injection is followed by a quiescent period of 7 hours, and followed by backflow at the same mass rate of 0.2 kg/s for 12 hours. At the end of the grid opposite the injection block, boundary conditions are maintained constant at their initial values. The heat exchange between fractures and rock matrix is modeled with the semi-analytical technique of Vinsome and Westerveld (1980). Thermal conduction in the wallrocks induced by cold water injection into the fractures is a multi-scale process, in which after time t the cooling front will penetrate to a depth of $x = \sqrt{D_{th} t}$. Fig. 2 shows the time-dependent depth of thermal penetration for a typical rock diffusivity of 0.8×10^{-6} m^2/s. The semi-analytical technique of Vinsome and Westerveld achieves an accurate representation of the multi-scale aspects of thermal conduction, while obviating the need for spatial discretization of the rock matrix. For comparison purposes and to track the hydrodynamic front, we co-inject a conservative solute tracer at a small concentration (mass fraction) of 10^{-5}; solute diffusion was neglected. The evolution of temperatures and solute concentrations through space and time was modeled with our general-purpose reservoir simulator TOUGH2 (Pruess, 2004).

Results for a case without wall rock present (fracture domain only) are given in Figs. 3-4. Spatial profiles of temperatures and solute tracer concentrations show some broadening (Fig. 3), which for the tracer is entirely due to numerical dispersion, while the temperature profile includes diffusive effects of heat conduction along the fracture. The centroid of the temperature profile at the end of the injection period is at a distance X = 4.405 m, while the solute tracer front is at X = 7.45 m, corresponding to a retardation factor of R_{th} = 7.45/4.405 = 1.69, in excellent agreement with the estimate of 1.66 derived above.

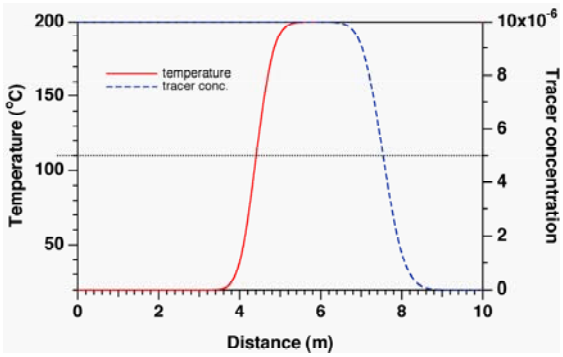

Figure 3: Spatial profiles of temperature and concentration of an inert tracer at the end of the injection period (5 hr). No wallrock present.

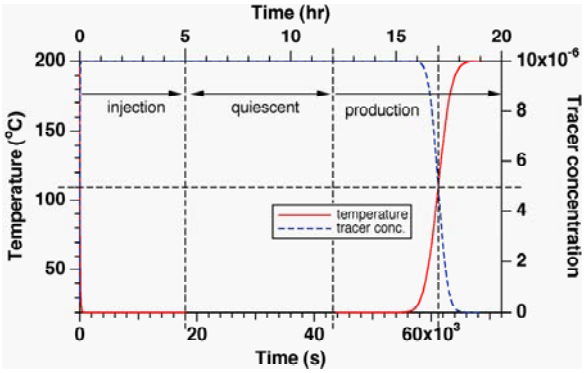

Figure 4: Simulated time dependence of temperatures and concentrations for an inert solute tracer; no wallrock present. Injection was made for 5 hours. Backflow at the same rate as injection commenced after a 7 hour quiescent period.

Fig. 4 shows return (backflow) curves for fluid temperature and solute concentration. Mid-point temperature (110 °C) and solute concentration (5×10^{-6}) occur after exactly 5 hr of backflow (17 hr total time), as they should. The temperature return

curve is noticeably broader than the curve for the solute tracer, reflecting diffusive effects from heat conduction along the fracture.

In order to explore the sensitivity of temperature returns to the available surface area for fracture-matrix heat transfer, we performed calculations that include wallrock for two different parametrizations of the fracture of (b, H) = (0.1 m, 10 m) and (0.02 m, 50 m), respectively (see Fig. 1). The two cases have the same cross-sectional area of bH = 1 m^2 for flow in the fracture domain, and are completely identical in all respects except for the fracture-matrix heat transfer area. Specific fracture-matrix interface area per unit length of the fracture is 20 m^2 for (b, H) = (0.1 m, 10 m) and is 100 m^2 for (b, H) = (0.02 m, 50 m). Results are given in Figs. 5-6, where the results previously obtained in the absence of fracture-matrix heat exchange are included as well for comparison.

Spatial profiles of temperatures at the end of the injection period show the expected effects (Fig. 5). Due to conductive heat transfer from the fracture walls, temperatures behind the position of the thermal

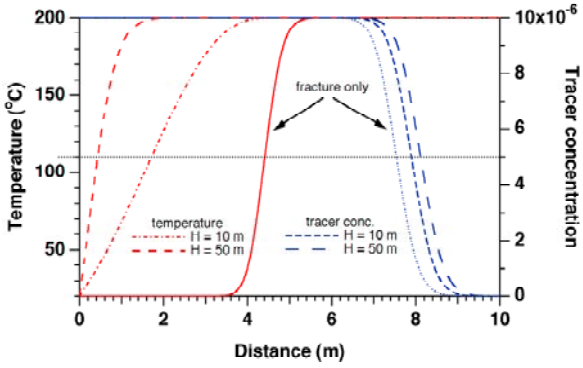

Figure 5: Spatial profiles of temperature and concentration of an inert tracer at the end of the injection period (5 hr) for different specific fracture-matrix interface areas.

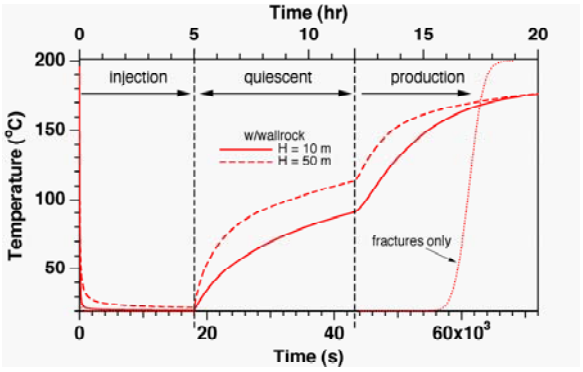

Figure 6: Simulated temperature returns for different specific fracture-matrix interface areas.

front for the cases with wallrocks are considerably higher, and more so for the taller, thinner fracture, that has five times larger specific surface area. The hydrodynamic fronts (inert solute tracer) are slightly more advanced than in the absence of wall rock, due to thermal expansion effects from generally higher fluid temperatures.

Conductive heating from the wallrocks produces dramatic changes in the temperature returns (Fig. 6). After shut-in of injection at t = 5 hr, temperatures begin to rise due to conductive heating locally, and more so for the taller fracture with larger specific rock surface area. The rate of temperature rise increases dramatically when backflow is initiated at t = 12 hr. At this time, fluid returned from the taller fracture (H = 50 m) has about 23 ^oC higher temperature, and subsequently shows a substantially faster recovery towards the original reservoir temperature of 200 ^oC.

CHARACTERIZING RESERVOIR STIMULATION

The goals of stimulation treatments are to (1) increase permeability (and porosity) of pre-existing fractures, and (2) create additional pathways for fluid flow by stimulating pre-existing fractures, as well as creating new ones. The chief objective of (1) is to facilitate flow through the fracture network, to increase flow rates and reduce pressure drop between injection and production sides. The objective of (2) is to expose additional rock surface area to injected fluids, and thereby increase the overall rate of heat transfer from rocks to fluids. In this section we present and discuss results of numerical simulation experiments that were designed to probe the ability of thermal SWIW tests to determine changes in reservoir parameters expected from stimulation treatments.

Increased Fracture Surface Area

Here we consider a hypothetical scenario in which stimulation enables injected fluid to access a second fracture with identical properties to the H = 50 m fracture considered previously. Injected fluid will then partition equally between the two fractures, reducing flow in each fracture to half the rate that was seen for the single-fracture case. Accordingly, the cooling rate in each fracture will be smaller than for the single-fracture case, and we expect higher temperatures during the backflow period. Fig. 7 shows that this is indeed the case. In the two-fracture system, the temperature at the injection point declines more slowly during the injection period than for a single fracture, and increases more rapidly during the quiescent period. At the beginning of the backflow period, the temperature at the injection point is approximately 7 ^oC higher than for a single fracture, and subsequent temperature recovery is somewhat

more rapid also. We emphasize that the simulation presented here was intended to explore basic effects; the test sequence of injection–quiescent period–production was not at all optimized to enhance the differences between the single- and two-fracture cases. We expect that test designs could be developed that would generate larger effects.

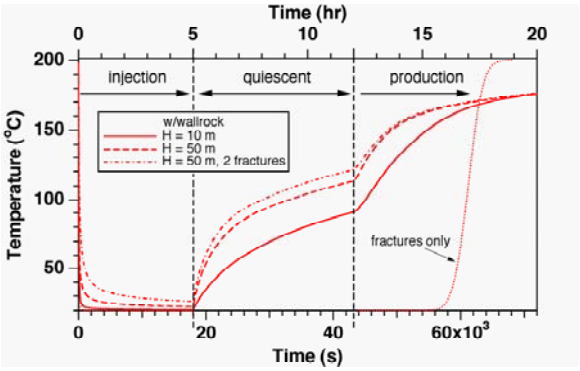

Figure 7: Simulated temperatures for different fracture-matrix systems.

Increased Effective Fracture Aperture

Here we consider a scenario of a single H = 50 m fracture with different apertures. The effective fracture aperture a is the product of the width b of the fracture domain and its intrinsic porosity ϕ, $a = b\phi$. It represents the fracture void volume per unit area. For numerical simulation, different a may be more conveniently realized by varying ϕ rather than b. Varying ϕ or b should make little difference as long as thermal equilibration over a distance b is rapid compared to time scales of interest in SWIW tests. Cases were run for intrinsic porosities of the fracture domain of ϕ = 25, 50, and 99 %, which for a width of the fracture domain of b = 2 cm corresponds to effective apertures of a = 0.5, 1, and 1.98 cm, respectively. Fig. 8 shows that the time dependence of temperatures is virtually identical for the three cases. This result is somewhat surprising, and may be understood as follows. When fluid is injected at a volumetric rate v_{inj}, the corresponding pore velocity $V_p = v_{inj}/(\phi bH)$ is inversely proportional to fracture aperture. Therefore, injected fluid will penetrate further into the fracture for smaller aperture, and will thus see a larger wallrock area for heat transfer. However, what matters for heat transfer is not the pore velocity of the fluid, but the velocity of the thermal front, which is given by

$$V_{th} = \frac{V_p}{R_{th}} = v_{inj}\frac{\rho_w c_w/bH}{\phi\rho_w c_w + (1-\phi)\rho_R c_R} \qquad (2)$$

where we have used Eq. (1) for thermal retardation. The groups $\rho_w c_w$ and $\rho_R c_R$ have comparable magnitude of approximately 4×10^6 and 2.65×10^6 J/m^3/°C, respectively, so that Eq. (2) for the velocity V_{th} of the thermal front depends only weakly on fracture porosity ϕ. This explains the results in Fig. 9, which show that simulated temperature profiles in the fracture at the end of the injection period are virtually identical for the different effective apertures, in spite of the substantial differences in pore velocities. For smaller effective fracture aperture, cooler temperatures do penetrate somewhat deeper into the fracture, but the differences are very small. Fig. 9 also includes a case with no wallrock in the fracture domain (ϕ = 100 %, b = 0.5 cm). For this case, cooling advances somewhat further into the fracture, but the differences are small. The temperature recovery from this case is virtually identical to the curves shown in Fig. 8.

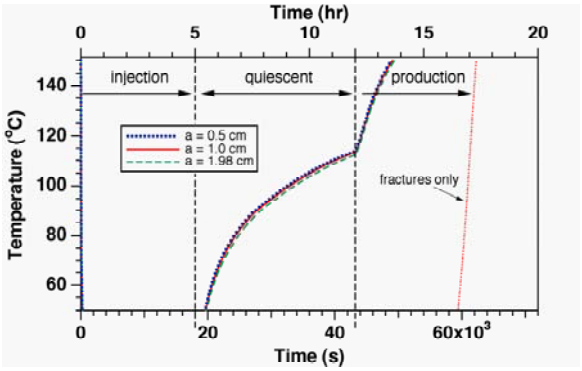

Figure 8: Simulated temperatures for different effective fracture apertures.

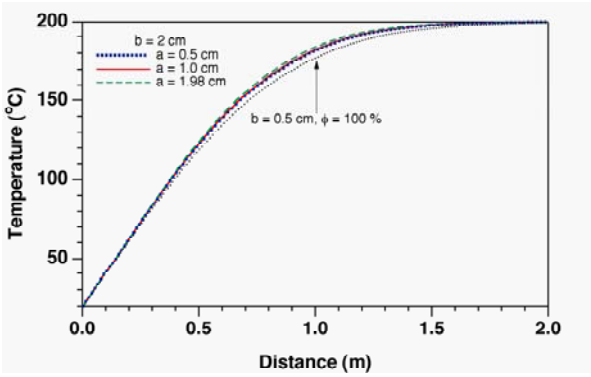

Figure 9: Simulated temperature profiles at the end of the injection period for fractures with different effective aperture. Injection rate was 0.2 kg/s for 18,000 s.

In an attempt to further clarify the underlying mechanisms, we modeled SWIW for fractures with a range of apertures, and using larger injection rates to change the relative time scales of fluid flow in the fracture and conductive heat transfer in the wallrocks. We expected that, if the same total amount of cold water was injected over a shorter time period, conductive heat transfer from the wallrocks would be

less able to heat the fluids in the fracture. This should generate cooler temperatures in the fracture to larger distance, and more so for smaller fracture aperture. This expectation was borne out by our simulations, but strong cooling effects could be generated only when injection rates were increased to very large values. Fig. 10 shows temperature profiles at the end of the injection period for a case in which injection rate was increased by a factor 500 to 100 kg/s. In these simulations, fracture permeability was also increased to limit pressure buildup at the injection point. The injection period in this case is only 36 s, as compared to 18,000 s in the earlier cases with an injection rate of 0.2 kg/s. We emphasize that such high rates and very brief injection periods do not correspond to a potentially realistic test design, but were used here in an effort to clarify the interplay between fluid flow in the fracture and conductive heat transfer in the wallrocks. As shown by Fig. 10, for such high rates and brief time periods heat conduction indeed is not able to "catch up" with fluid flow, and substantially colder temperatures now penetrate much further into the fracture. Also, the expected effect of deeper cooling for smaller aperture (larger pore velocity) is observed, although this effect is much weaker than might be expected from the 1:2 ratio of pore velocities. In spite of the significant differences in temperature profiles at the end of the injection period seen in Fig. 10, temperature changes over time are virtually identical (Fig. 11) throughout the entire quiescent period (here extending to 18 hr), and the subsequent withdrawal period (here at a rate of 1 kg/s, so that all injected fluid is back-produced at t = 19 hr). These results suggest that temperature returns from thermal SWIW are insensitive to changes in fracture apertures.

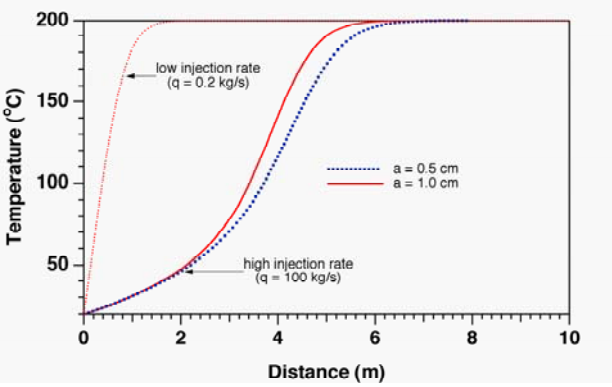

Figure 10: Simulated temperature profiles for injection at a very high rate of 100 kg/s at the end of the injection period (36 s), for a fracture with H = 50 m and two different effective apertures. The case of injecting the same amount of water at a low rate is included for comparison.

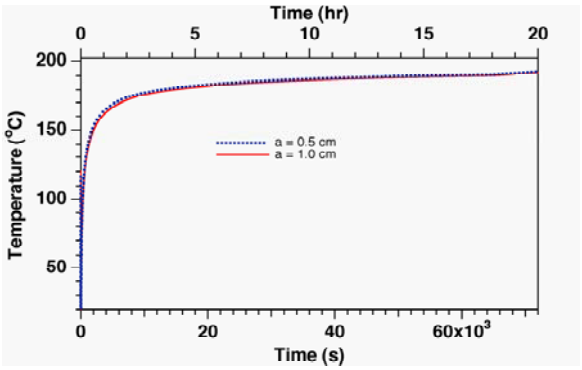

Figure 11: Simulated temperature returns following cold water injection at 100 kg/s into fractures with two different effective apertures.

CONCLUDING REMARKS

The main reservoir improvements targeted with stimulation treatments involve (1) exposing additional rock surface area to fluids circulating in the fracture network, and (2) improving flow capacity of existing fractures. The first goal aims to increase heat transfer rates, while the second aims to increase mass flows. Single-well injection-withdrawal (SWIW) tests using temperature as tracer may offer interesting possibilities for characterizing reservoir fracture parameters and for determining their changes in response to stimulation treatments.

An advantage of using temperature as a tracer is that thermal parameters have much less variability than chemical parameters for reversibly sorbing aqueous solutes. In addition, thermal diffusivities are 4-5 orders of magnitude larger than diffusivities of solutes in typical low-permeability matrix rocks with microdarcy permeability. These features provide for a strong and robust signal from fracture-matrix heat exchange. Our limited numerical simulation experiments indicate that exposure of additional rock surface area to fluids circulating in the fractures provides a significant response in thermal SWIW tests. An increase in exposed rock surface area yields higher rates of heat transfer, and leads to higher temperatures and more rapid temperature recovery during backflow.

Increases in effective fracture aperture from stimulation activities had been expected to generate a strong signal of lower temperature returns, based on the fact that the heat transfer area seen by a given amount of injected fluid is inversely proportional to fracture aperture. However, our simulations indicate that *in situ* temperature profiles at the end of the injection period are quite insensitive to fracture porosity, which explains why SWIW returns are not sensitive to changes in fracture porosity either. These findings are preliminary and suggest that, for the

parameter specifications explored in the present study, evolution of temperatures is dominated by conductive heat exchange between injected fluids and fracture wall rocks. The insensitivity of temperature returns to effective fracture aperture represents both bad news and good news. The bad news is that thermal SWIW cannot discern inflation of existing fractures from stimulation treatments. The good news is that the lack of sensitivity to fracture apertures and their changes will make it easier to distinguish the thermal signature of additional heat transfer area.

ACKNOWLEDGMENT

Thanks are due to Tianfu Xu for a review of the manuscript. We appreciate stimulating discussions with Tianfu Xu and Pete Rose, and helpful comments from Grimur Bjornsson. This work was supported by the Assistant Secretary for Energy Efficiency and Renewable Energy, Office of Technology Development, Geothermal Technologies Program, of the U.S. Department of Energy under Contract No. DE-AC02-05CH11231.

REFERENCES

Bjornsson, G. Reservoir Conditions at 3-6 km Depth in the Hellisheidi Geothermal Field, SW-Iceland, Estimated by Deep Drilling, Cold Water Injection and Seismic Monitoring, *Proceedings*, Twenty-Ninth Workshop on Geothermal Reservoir Engineering, Stanford University, Stanford, California, January 26–28, 2004.

Bodvarsson, G. Thermal Problems in the Siting of Reinjection Wells, *Geothermics*, Vol. 1, No. 2, pp. 63–66, 1972.

Doughty, C. and C.-F. Tsang. Analysis of Three Sets of SWIW Tracer-test Data Using a Two-population Complex Fracture Model for Diffusion and Sorption, Lawrence Berkeley National Lab., Berkeley, CA, July, 2009.

Ghergut, I., C.M. Dermott, M. Sauter, M. Herfort and O. Kolditz. Reducing Ambiguity in Fractured-Porous Media Characterization Using Single-Well Tracer Tests, in *ModelCARE-2005: From Uncertainty to Decision Making*, K. Kovar, M. F. P. Bierkens, H. Gehrels (editors), IAHS Red Book no. 304, Wallingford, 2006.

Ghergut, I., M. Sauter, H. Behrens, T. Licha, T. Tischner and R. Jung. Single-Well Dual-Tracer Spikings during EGS Creation in Northern German Sedimentary Layers, *Proceedings*, Thirty-Fourth Workshop on Geothermal Reservoir Engineering, Stanford University, Stanford, California, February 9-11, 2009.

Haggerty, R., S.W. Fleming, L.C. Meigs and S.A. McKenna. Tracer Tests in a Fractured Dolomite, 2. Analysis of Mass Transfer in Single-Well Injection-Withdrawal Tests, *Water Resour. Res.*, Vol. 37, No. 5, pp. 1129–1142, May 2001.

Kocabas, I. and R.N. Horne. Analysis of Injection-Backflow Tracer Tests im Fractured Geothermal Reservoirs, *Proceedings*, Twelfth Workshop on Geothermal Reservoir Engineering, Stanford University, Stanford, California, January 1987.

Kohl, T., K.F. Evans, R.J. Hopkirk and L. Rybach. Coupled Hydraulic, Thermal, and Mechanical Considerations for the Simulation of Hot Dry Rock Reservoirs, *Geothermics*, Vol. 24, No. 3, pp. 345 - 359, 1995.

Kohl, T. and T. Mégel. Predictive Modeling of Reservoir Response to Hydraulic Stimulations at the European EGS Site Soultz-sous-Forêts, *Int J. Rock Mech. Min. Sci.*, Vol. 44, pp. 1118–1131, 2007.

Nalla, G. and G.M. Shook. Novel Application of Single-Well Tracer Tests to Evaluate Hydraulic Stimulation Effectiveness. *GRC Transactions*, September 2005.

Neretnieks, I. and L. Moreno. Prediction of some in situ Tracer Tests with Sorbing Tracers Using Independent Data, *J. Contam. Hydr.*, Vol. 61, pp. 351–360, 2003.

Neretnieks, I. Single Well Injection Withdrawal Tests (SWIW) in Fractured Rock - Some Aspects on Interpretation, Report R-07-54, Department of Chemical Engineering and Technology, Royal Institute of Technology, Stockholm, Sweden, August 2007.

Pruess, K. Numerical Simulation of Multiphase Tracer Transport in Fractured Geothermal Reservoirs, *Geothermics*, Vol. 31, pp. 475 - 499, 2002.

Pruess, K. The TOUGH Codes—A Family of Simulation Tools for Multiphase Flow and Transport Processes in Permeable Media, *Vadose Zone J.*, Vol. 3, pp. 738 - 746, 2004.

Pruess, K., T. van Heel and C. Shan. Tracer Testing for Estimating Heat Transfer Area in Fractured Reservoirs, *Proceedings*, World Geothermal Congress 2005, Antalya/Turkey, April 2005.

Sanjuan, B., J.-L. Pinault, P. Rose, A. Gérard, M. Brach, G. Braibant, C. Crouzet, J.-C. Foucher, A. Gautier and S. Touzelet. Tracer Testing of the Geothermal Heat Exchanger at Soultz-sous-Forêts (France) between 2000 and 2005, *Geothermics*, Vol. 35, No. 5-6, pp. 622–653, 2006.

Shan, C. and K. Pruess. An Analytical Solution for Slug Tracer Tests in Fractured Reservoirs, *Water*

Resour. Res., Vol. 41, W08502, doi:10.1029/2005WR004081, 2005.

Shook, G.M. Predicting Thermal Breakthrough in Heterogeneous Media from Tracer Tests, *Geothermics*, Vol. 30, No. 6, pp. 573–589, 2001.

Tulinius, H., G. Axelsson, J. Tómasson, H. Kristmannsdóttir and A. Gudmundsson, *Proceedings*, Tweenty-first Workshop on Geothermal Reservoir Engineering, Stanford University, Stanford, California, January 22–24, 1996.

Vinsome, P.K.W. and J. Westerveld. A Simple Method for Predicting Cap and Base Rock Heat Losses in Thermal Reservoir Simulators, *J. Canadian Pet. Tech.*, 19 (3), 87–90, July-September 1980.

Witherspoon, P.A., J.S.Y. Wang, K. Iwai, and J.E. Gale. Validity of Cubic Law for Fluid Flow in a Deformable Rock Fracture, *Water Resour. Res.*, Vol. 16, No. 6, pp. 1016 - 1024, 1980.

Xu, T., P. Rose, S. Fayer and K. Pruess. On Modeling of Chemical Stimulation of an Enhanced Geothermal System Using a high pH Solution with Chelating Agent, *Geofluids*, Vol. 9, No. 2, pp 167–177, 2009.